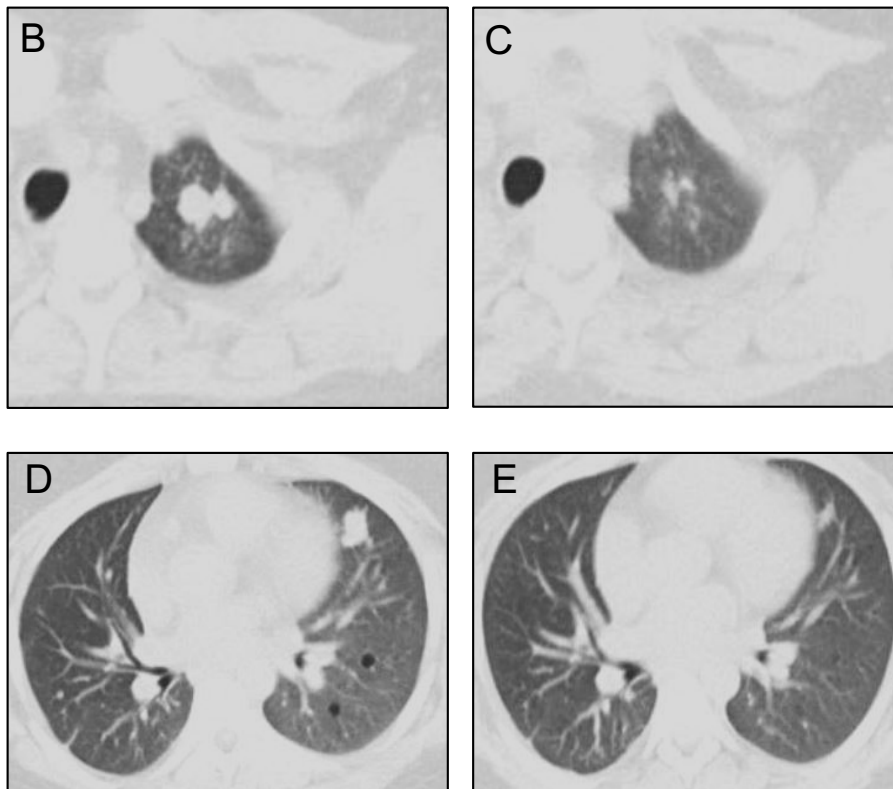


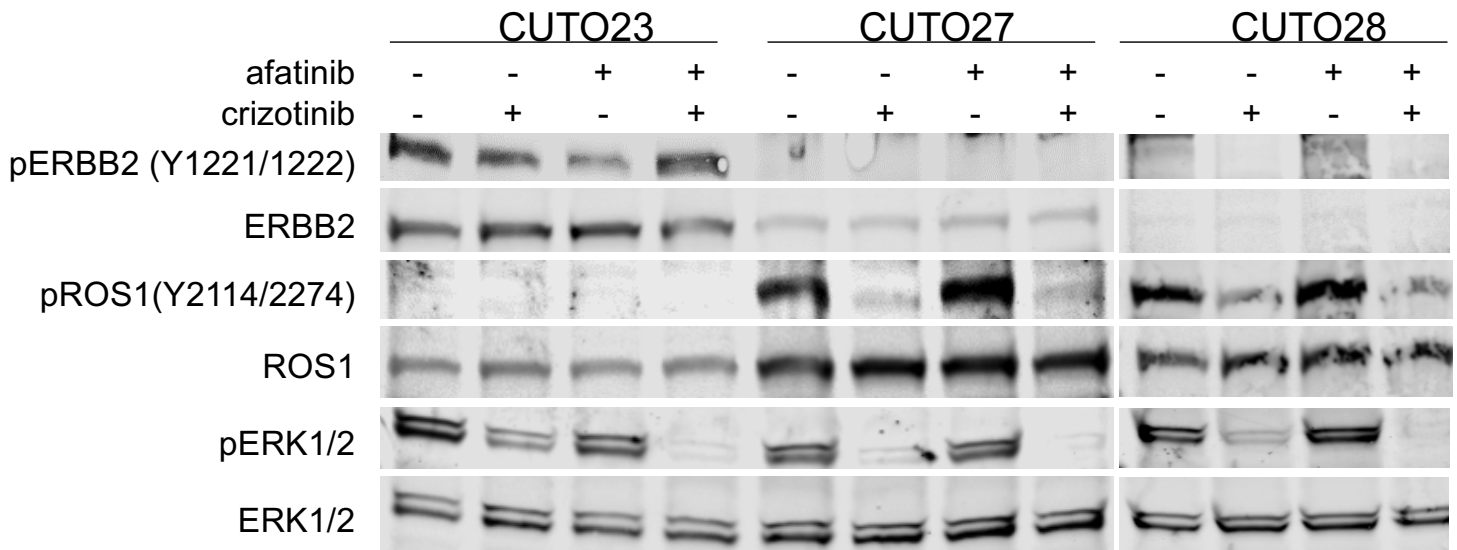
A

*EML4* [exon 17] *ALK* [exon 20]  $\Delta$ 79NT  
 GCCATAGGAACGCACTCAGGCagacggagctctgctctgctgcccaggctggagtcagtgggcgcaatctcggtcactgCACCTCGACCATCATGACCGACTACAACC  
*EML4* [intron 17]

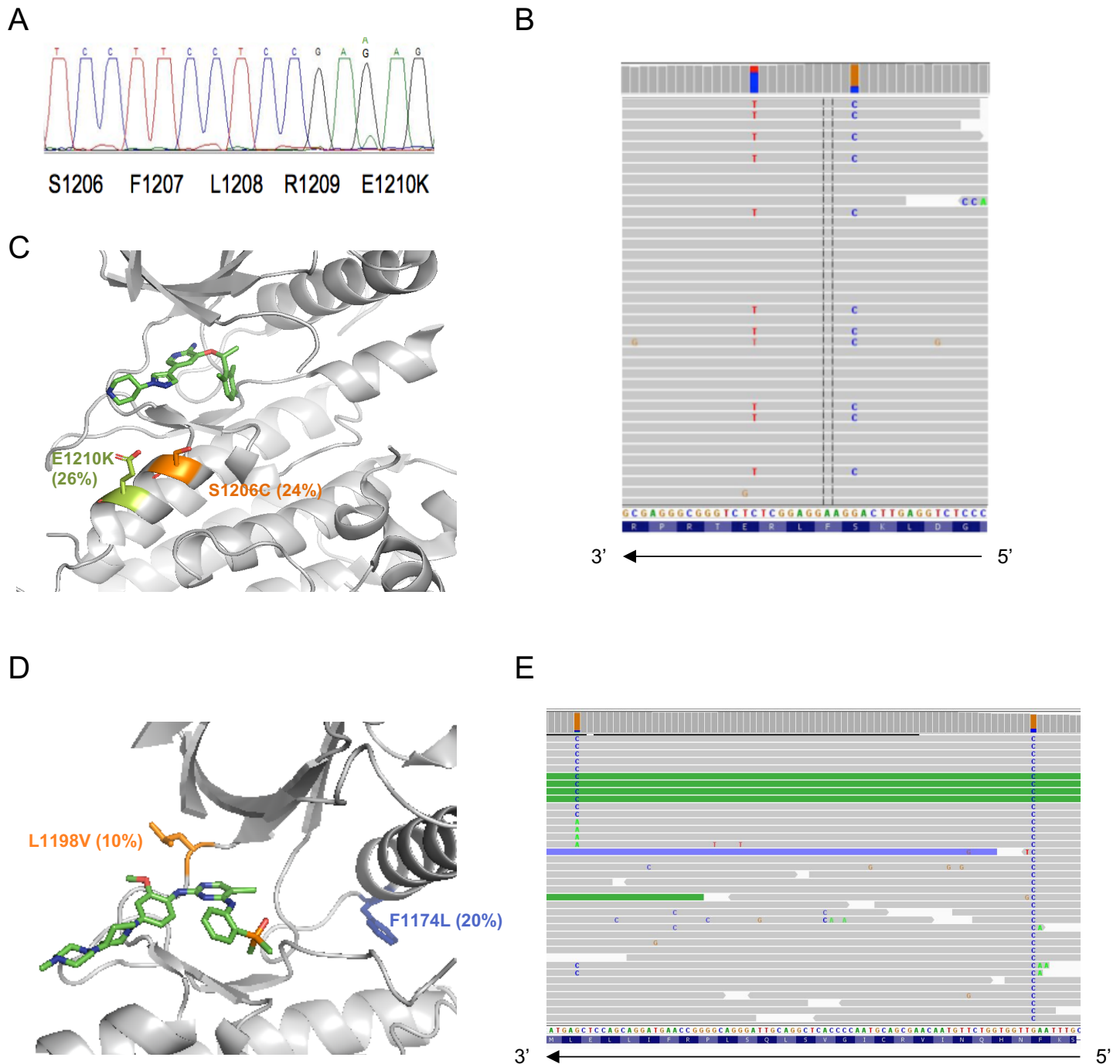


**Supplementary Figure 1. Case example of an ALK + patient response to alectinib.**

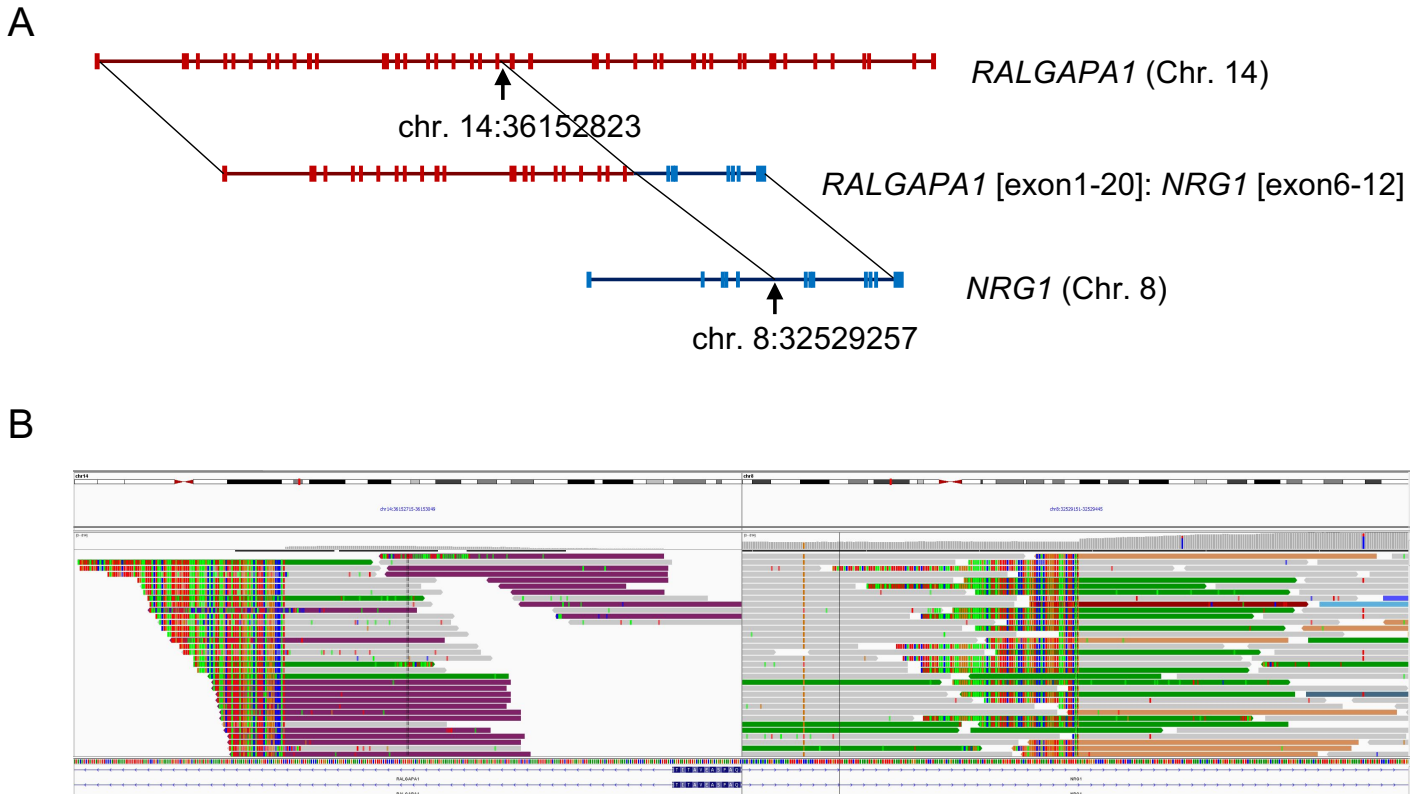
The patient was diagnosed with ALK+ NSCLC (E17:A20). **A**, RNA sequence demonstrates the fusion transcript of *EML4* exon 17 and sequences derived from *EML4* intron 17 and is lacking the first 79 nucleotides from exon 20 of *ALK*. **B-E**, Representative axial CT scan images demonstrate significant responses to alectinib in two areas which are representative of total disease burden. **B and D**, Pre-alectinib CT scan images. **C and E**, CT images following 11 weeks of treatment with alectinib 600mg twice daily demonstrate disease response.



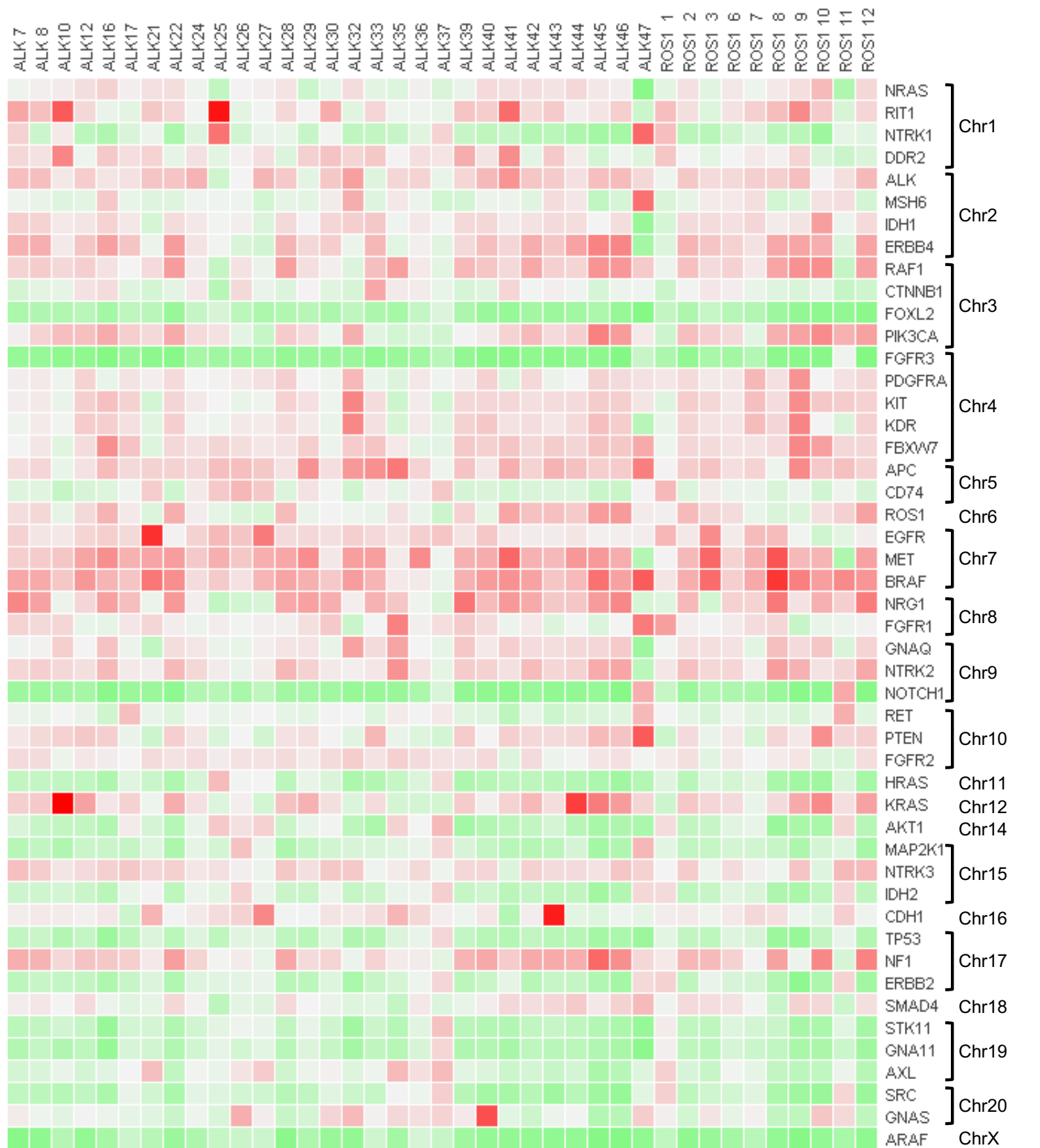
**Supplementary Figure. 2. HER2 is activated in the ROS1+ CUTO23 cell line compared to ROS1 inhibitor sensitive cell lines.** Western blot analysis of CUTO23, CUTO27, and CUTO28 cell lines demonstrating increased total and phosphorylated HER2 (ERBB2) in CUTO23 compared with CUTO27 and CUTO28. Cells were also treated in the absence or presence of the ROS1 inhibitor crizotinib (500 nM) and the pan-HER inhibitor afatinib (100nM) for 2 hours demonstrating inhibition of pERBB2 with afatinib and concomitant rescue of inhibition of downstream signaling by ERK1/2 with the addition of afatinib to crizotinib in CUTO23 cells. Notably, ROS1 but not pROS1 is observed in CUTO23, whereas CUTO27 shows both total and phosphorylated ROS1. CUTO23 and CUTO27 both harbor the *CD74-ROS1* gene fusion, whereas CUTO28 harbors a *TPM3-ROS1* fusion.



**Supplementary Figure 3. Post-brigatinib ALK+ tumor samples with compound mutations *in cis*.** **A**, Direct sequencing of PCR product (gDNA) from post-crizotinib sample (ALK-29\_1) showing a small peak indicating a sub-clonal population containing the ALK E1210K KDM. **B**, NGS of post-brigatinib sample (ALK-29\_2) demonstrating a double ALK S1206C/E1210K KDM *in cis*. **C**, Crystal structure of crizotinib bound to ALK [PDB 2XP2]. ALK S1206C/E1210K with variant allele frequencies (VAF) shown in parentheses for each mutation. **D**, Crystal structure of brigatinib bound to ALK [PDB 5J7H] demonstrating the compound ALK F1174V and L1198V with variant allele frequencies (VAF) shown in parentheses for each mutation. **E**, NGS of post-brigatinib sample (ALK-44\_2) demonstrating ALK F1174V single mutation or F1174V/L1198V KDM *in cis*.



**Supplementary Figure 4. *RALGAPA1-NRG1* fusion induces resistance in ALK+ cancer.** **A**, Genomic structure of the introns and exons for human *RALGAPA1* [NG\_051667.1 RefSeqGene] (red) and human *NRG1* [NG\_012005.2 RefSeqGene] (blue) with the genomic breakpoint coordinates according to GRCh37/hg19. **B**, Screen capture from the Integrative Genomics Viewer (IGV) showing the breakpoint-spanning sequencing reads for the *NRG1* and *RALGAPA1* loci acquired from our hybrid capture NGS assay.



-2  
COPY\_NUMBER

0

2

**Supplemental Figure 5. Copy Number Variation.** Heatmap illustrating relative copy number for the 48 genes in custom NGS panel. Genes are arranged by chromosome.